Phys. Status Solidi B **252**, No. 5, 1089–1095 (2015) / **DOI** 10.1002/pssb.201451571

physica status solidi b
www.pss-b.com
basic solid state physics

Growth of high-quality AlN layers on sapphire substrates at relatively low temperatures by metalorganic chemical vapor deposition

Xiao-Hang Li*[,1], Shuo Wang[2], Hongen Xie[2], Yong O. Wei[2], Tsung-Ting Kao[1], Md. Mahbub Satter[1], Shyh-Chiang Shen[1], Paul Douglas Yoder[1], Theeradetch Detchprohm[1], Russell D. Dupuis[1], Alec M. Fischer[2], and Fernando A. Ponce[2]

[1] Center for Compound Semiconductors and School of Electrical and Computer Engineering, Georgia Institute of Technology, Atlanta, Georgia 30332, USA
[2] Department of Physics, Arizona State University, Tempe, Arizona 85287, USA

Received 27 September 2014, revised 14 November 2014, accepted 1 December 2014
Published online 21 January 2015

Keywords AlN, laser diodess, MOCVD, III-nitride semiconductors, optically pumped lasers, sapphire

* Corresponding author: e-mail xli@gatech.edu, Phone: +01 404 385 6094, Fax: +01 404 385 6096
** e-mail dupuis@gatech.edu, Phone: +01 404 385 6094, Fax: +01 404 385 6096

We report a three-step method to grow high-quality AlN heteroepitaxial layers on sapphire substrates at relatively low temperatures by metalorganic chemical vapor deposition (MOCVD) without the use of epitaxial lateral overgrowth (ELO) or pulse atomic layer epitaxy (PALE) method. The three-layer AlN structure comprises a 15-nm thick buffer layer, a 50-nm thick intermediate layer, and a 3.4-μm thick template layer grown at 930, 1130, and 1100 °C sequentially on the *c*-plane sapphire substrate. The resulting AlN layer had smooth surface with well-defined terraces and low root-mean square (RMS) roughnesses of 0.50 and 0.07 nm for 20×20 and $1 \times 1\ \mu m^2$ atomic force microscopy (AFM) scans. Band-edge emission was observed at 208 nm by room temperature (RT) photoluminescence (PL) measurements. The total threading dislocation density was $2.5 \times 10^9/cm^2$ as determined by transmission electron microscopy (TEM), which is comparable to those of some AlN layers recently grown at significantly higher temperatures. Growth evolution was studied and correlated to the TEM results. The residual impurity concentrations were comparable to those of AlN layers grown at higher temperatures, *i.e.*, 1200–1600 °C. This study demonstrates the high quality AlN layers on sapphire substrates can be grown at achievable temperatures for most of the modern MOCVD systems.

1 Introduction III-nitride deep-ultraviolet (DUV) emitters including light-emitting diodes (LEDs) and laser diodes (LDs) have applications in important areas including disinfection and digital data storage. Bulk AlN substrates are ideal for the growth of DUV emitters due to the low-dislocation density, reduced lattice, and thermal mismatch with high-Al content AlGaN [1]. However, the use of these substrates is constrained by issues like limited supply, high cost, DUV absorption, and small substrate size. Therefore, currently commercialization of III-nitride DUV emitters relies on the use of AlN layers grown on lower-cost, DUV-transparent, and relatively larger foreign substrates, especially *c*-plane sapphire substrates. However, the large lattice and thermal mismatch leads to a high dislocation density in the AlN layers. The performance of III-nitride DUV emitters is very sensitive to the dislocation-related non-radiative recombination centers [2, 3], hence it is crucial to reduce the dislocation density of AlN layers.

A common approach to reducing the dislocation density in the growth of heteroepitaxial layers is the use of epitaxial lateral overgrowth (ELO), where AlN layers are regrown on patterned seeding AlN layers [4–7]. However, because the ELO approach involves fabrication like etching as well as a regrowth process of the many-μm thick layer to coalesce over the patterned layers, it is associated with higher cost and longer processing time, uneven surfaces, and growth complexity. Another approach, the pulsed atomic layer epitaxy (PALE) process, where N and/or Al sources are supplied in a pulsed mode to allow Al atoms additional time to mobilize on the epitaxial surface has been used [3, 8, 9]. In

some studies, the ELO and PALE were collectively employed to expedite the coalescence over the patterned layers [5, 7].

In addition to the ELO and PALE, high-temperature growth above 1200 °C has been employed independently or collectively with the ELO and PALE to achieve low dislocation density and smooth surface morphology by metalorganic chemical vapor deposition (MOCVD), where the mobility of Al atoms on the epitaxial surface is enhanced at high temperatures [10–17]. However, there are concerns regarding the high-temperature growth. Not only does it require a special reactor configuration and/or reactor parts to reach and maintain high temperatures, but it can also cause considerable thermal stress in the heteroepitaxial layer due to the large thermal expansion mismatch between the AlN layers and sapphire [18]. In addition, the serious wafer bowing at high temperature can deteriorate wafer uniformity such as the layer thickness and the composition of layers grown on the AlN layers [19, 20]. To address these issues, there have been some attempts to grow AlN layers on sapphire [21] and SiC [22] substrates below 1200 °C. However, the surface of these AlN layers was found to suffer from a high density of defects [21, 22]. Thus there have been few successful studies of growing high-quality planar AlN layers on the sapphire substrates below 1200 °C. Recently, a detailed temperature dependence study indicated that the Al atom mobility was adequate to achieve coalesced and smooth surface at temperatures as low as 1086 °C without the use of ELO or PALE [23]. Hence the planar AlN layers with high quality may be obtainable at such temperatures.

In this work, we developed a simple recipe to grow high-quality AlN layers at relatively-low growth temperatures up to 1130 °C, which are accessible for most of the modern III-nitride MOCVD systems. Details of the growth process and characterization are presented hereafter. Neither the ELO nor PALE approach was used in this study. The crystalline quality of AlN layers was assessed by scanning electron microscopy (SEM), atomic force microscopy (AFM), X-ray diffraction (XRD), photoluminescence (PL), transmission electron microscopy (TEM), and secondary ion mass spectroscopy (SIMS).

2 Experimental details The AlN heteroepitaxial structure comprised three layers grown under different conditions. The MOCVD system we used was an AIXTRON $3 \times 2''$ close-coupled-showerhead (CCS) system. The emissivity-corrected surface temperature was measured by a dual-wavelength multiple-point pyrometric profiling system. Trimethylaluminum (TMAl) and ammonia (NH_3) were used as precursors and hydrogen (H_2) as carrier gas. The total flow rates of precursors and carrier gas were kept constant at 20 slm. Prior to the AlN growth, the susceptor and sapphire substrates were baked at 1100 °C for 5 min in a H_2 ambient. A dose of 0.57 μmol of TMAl was deposited at 930 °C after the bake to pre-condition the sapphire surface for growing Al-polar AlN layers [24].

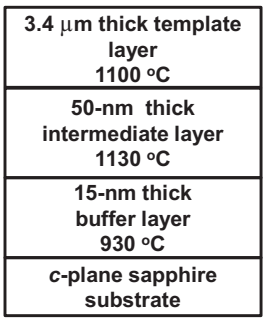

Figure 1 Cross-sectional schematic diagram of the three-layer AlN/sapphire structure with corresponding growth temperatures.

As shown in Fig. 1, the growth started with a 15-nm thick AlN buffer layer grown at 930 °C with a V/III ratio of 1500 on a 2-inch diameter *c*-plane sapphire substrate with an offcut angle of 0.2° toward *m*-plane. Afterwards, a 50-nm thick AlN intermediate layer was deposited at 1130 °C with a V/III ratio of 74 for a short growth period of 100 s. The importance of the AlN intermediate layer is discussed in Section 3. The growth was concluded by depositing a 3.4-μm thick AlN template layer grown at 1100 °C at a V/III ratio of 66. The reactor pressure was set at 85 mbar (64 Torr) during the growth of the AlN layers. Growth rate of the template layer was 2.3 μm/h or 0.64 nm/s, which is considered to be relatively fast for AlN growth by MOCVD. Based on the supplying molar flow of TMAl and growth rate, growth efficiency of the AlN template layer was calculated to be 2134 μm/mol, or 36% of the injected TMAl molecules was effectively incorporated to grow the AlN template layer. This growth efficiency is thus similar to that of a previous study using an extremely low V/III ratio of 10 to grow AlN layers efficiently [25].

3 Results and discussion The SEM image in Fig. 2 exhibits surface morphology of the AlN/sapphire structure. Neither pits nor hillocks were visible, indicating a smooth surface because of good coalescence and two-dimensional (2D) growth even at relatively low growth temperatures. To investigate the evolution of surface morphology, the growth

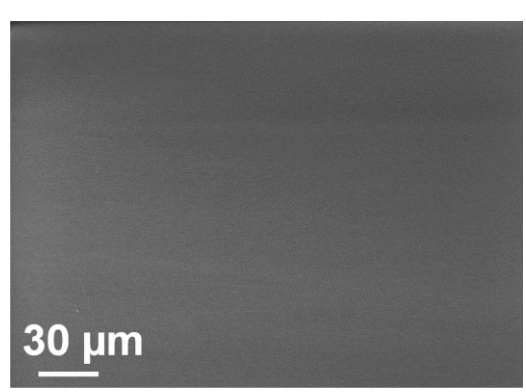

Figure 2 Oblique-view SEM image for surface morphology of the three-layer AlN/sapphire structure.

was interrupted at different stages and the surface morphology was observed by AFM as shown in Fig. 3(a–h). Each figure corresponds to a sample grown independently on a sapphire substrate to avoid defect formation from a regrown surface, and contamination induced during the measurement. As shown in Fig. 3(a), three-dimensional (3D) growth dominated in the lowest-temperature buffer layer with lateral island dimensions of around 100 nm. With further growth of the 50-nm AlN intermediate layer at 1130 °C, the surface morphology started to shift from 3D to 2D, as shown in Fig. 3(b). By switching to growth of the final AlN template layer at 1100 °C, the transition from 3D to 2D growth modes continued and the surface began to planarize as shown in Fig. 3(c–f).

Surface pits caused by uncoalesced islands were still seen at a total thickness of 1.40 μm where atomic steps started to become visible. However, the pit density in Fig. 3 (f) is significantly reduced compared to those in Fig. 3(a–e), indicating proximity to the complete coalescence. With a thicker AlN template layer, the surface pits disappeared at a total thickness of 2.80 μm as shown in Fig. 3(g). In Fig. 3(g), some threading dislocations appearing as surface point defects marked by arrows were visible at the coalescence points as step terminations. In Fig. 3(h) the surface of complete AlN/sapphire structure, and well-defined steps and terraces are observed, indicating an Al-polar surface with dominant 2D step-flow growth. The height difference between terraces is in the range of 0.20–0.30 nm corresponding to one monolayer of (0001) AlN ($c/2 = \sim 0.25$ nm). Root-mean-square (RMS) roughness is 0.07 nm, which is comparable with that of some polished bulk AlN substrates [26]. Thus the heteroepitaxial growth of AlN layers on sapphire at temperatures ~1100 °C can provide smooth surfaces for the subsequent deposition of III-nitride layers on top. In addition, the threading dislocation density on surface is greatly reduced as compared to Fig. 3(g), suggesting that the threading dislocations continued to bend with an increased layer thickness after the surface was fully coalesced.

Room-temperature PL and XRD were used to characterize the samples presented in Fig. 3(a–h), as shown in Fig. 4 and Table 1. The top-surface-emitted PL spectra were obtained via optically pumping the samples by a pulsed ArF excimer laser ($\lambda = 193$ nm) with a pumping power density of 2.7 MW/cm^2. Details of the optical pumping experiment setup can be found elsewhere [1]. In Fig. 4, high-energy spectral tails at $\lambda < 205$ nm were from the unabsorbed pumping laser emission. As shown in Fig. 4, no considerable emission is seen for the samples with total thicknesses of 15 and 65 nm corresponding to the completion of buffer and intermediate layers with broad (002) and (102) FWHMs shown in Table 1, indicating very low radiative efficiency. The band-edge emission begins to be seen at 210.9 nm from the sample with a total thickness of 200 nm and reduced (002) and (102) FWHMs of 1908 and 2783 arcsec. The PL emission intensity generally increased with the thickness and smaller (002) and (102) FWHMs, which implies enhanced

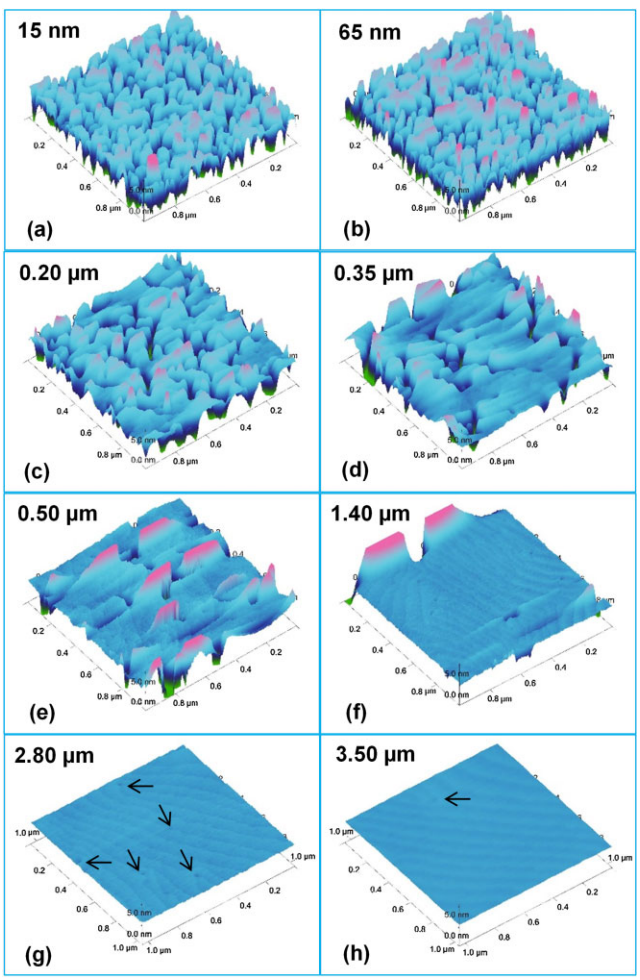

Figure 3 (a–h) $1 \times 1\ \mu m^2$ AFM images showing surface morphology evolution of the three-layer AlN/sapphire structure as a function of total AlN layer thickness shown on the upper left corner of each figure. Figure 3(h) corresponds to the complete sample structure where the RMS roughness is 0.07 nm.

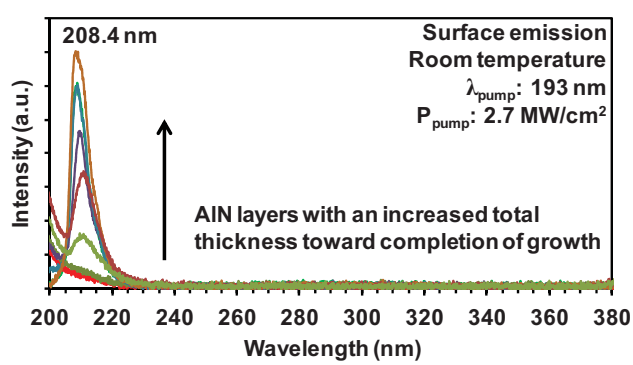

Figure 4 Room-temperature PL spectra of the AlN/sapphire structure with different total layer thicknesses toward growth completion, corresponding to Fig. 3(a–h). The spectral curves of the 1.40 μm and 2.80 μm thick AlN samples overlap each other, which may be due to similar radiative efficiency.

Table 1 FWHMs of XRD (002) and (102) ω-scans as well as PL characteristics of the three-layer AlN/sapphire structure as a function of total thickness through the growth evolution.

total thickness (μm)	corresponding AFM figure	(002) FWHM arcsec	(102) FWHM arcsec	PL peak λ (nm)	PL FWHM (nm)
0.015	Figure 3(a)	3107	4266	NA	NA
0.065	Figure 3(b)	2581	3899	NA	NA
0.20	Figure 3(c)	1908	2783	210.9	12.0
0.35	Figure 3(d)	1548	1987	210.9	9.6
0.50	Figure 3(e)	1138	1670	209.7	6.2
1.40	Figure 3(f)	601	914	208.9	6.2
2.80	Figure 3(g)	349	659	208.9	5.9
3.50	Figure 3(h)	280	480	208.4	6.9

radiative efficiency due to reduced dislocation densities. Despite different thicknesses, the spectral curves of the 1.40 μm- and 2.80 μm-thick AlN samples overlap each other, which may be due to similar radiative efficiency. The smallest (002) and (102) the XRD FWHMs are 280 and 480 arcsec, suggesting relatively low mosaicity and dislocation density. The spectral FWHM decreases to as narrow as 5.9 nm for a total AlN thickness of 2.80 μm. Then it increases to 6.9 nm probably caused by a secondary bound-exciton peak [16] for the AlN/sapphire structure with a total thickness of 3.50 μm. In addition, a blueshift in peak wavelength with increased peak intensity is observed with the shortest peak wavelength of 208.4 nm for the complete structure, which can be attributed to the increased compressive strain with a larger thickness [27]. There is no considerable deep level emission up to 380 nm, indicating low density of deep-level recombination centers.

To determine the dislocation density of complete AlN three-layer AlN/sapphire structure, TEM samples for cross-sectional and plan-view imaging were prepared by mechanically wedge-polishing techniques, followed by Ar ion milling at 3.5 keV. The microstructure of AlN layers was studied using a JEOL 4000EX TEM operating at 400 kV. Figure 5(a–b) show dark-field cross-sectional TEM images under the two-beam condition with $\boldsymbol{g} = 0002$ and $11\bar{2}0$, respectively. The plan-view image was taken under diffraction condition with $\boldsymbol{g} = 11\bar{2}0$. The sample was intentionally titled away from the zone axis to project the threading dislocations as segments in the image. Since the dislocations seen in Fig. 5(a) were also visible in Fig. 5(b), it is suggested that there was no pure screw dislocation, and thus the dislocations observed in Fig. 5(a) were of mixed type instead. The densities of mixed and edge dislocations near the epitaxial surface as analyzed from Fig. 5(a–b) are

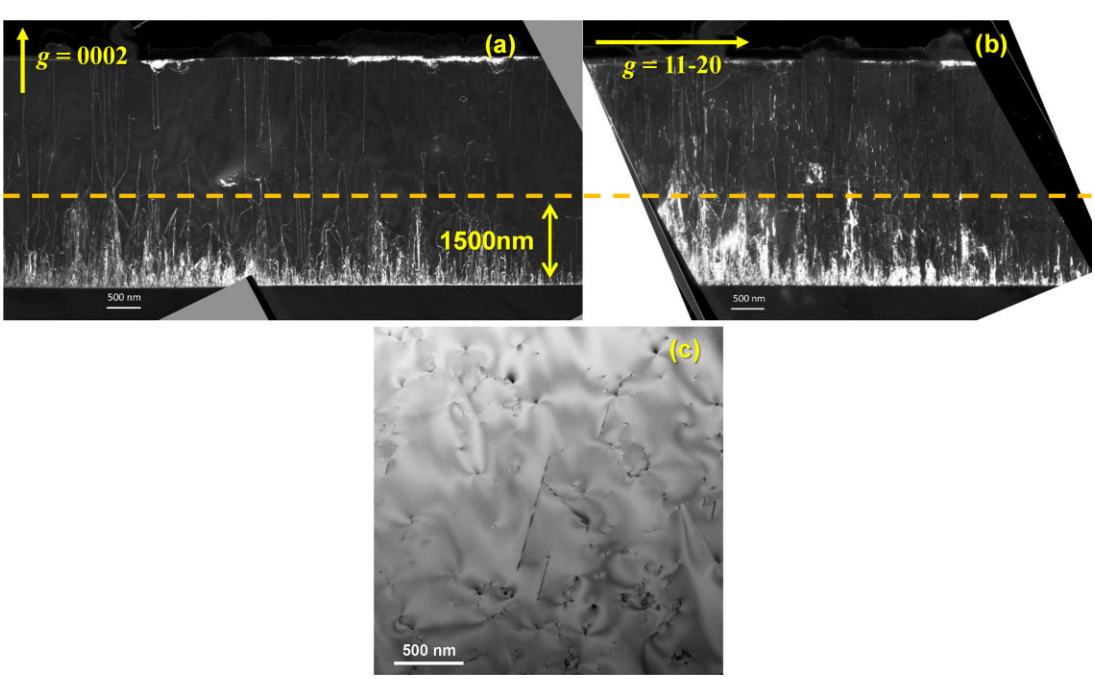

Figure 5 Dark-field cross-sectional TEM images with (a) $\boldsymbol{g} = 0002$ and (b) $\boldsymbol{g} = 11\bar{2}0$, wherein the orange dashed line shows approximately where most of the dislocations were annihilated, and (c) plan-view TEM image of the three-layer AlN/sapphire structure.

1.0×10^9 and $1.5 \times 10^9\,cm^{-2}$, respectively. Hence the total dislocation density is $\sim 2.5 \times 10^9/cm^2$, which agrees with the plan-view TEM experiment as shown in Fig. 5(c). Thus, the total dislocation density is comparable to those of some recent studies where the AlN layers were grown on sapphire substrates at temperatures above 1300 °C by taking into account the thickness difference [3, 12, 15].

The cross-sectional TEM images in Fig. 5(a–b) were further compared with TEM analysis results in the previous studies regarding the growth of high-quality AlN layers on sapphire substrates [11, 12, 13, 15]. In those studies where temperatures higher than 1300 °C were employed, most of the dislocations were annihilated at a thickness of less than 500 nm from the AlN/sapphire interface. However, as shown in Fig. 5(a–b), most of the dislocations were gradually removed and finally annihilated at larger thicknesses of 1000–1500 nm from the AlN/sapphire interface as marked by the yellow dashed line. This thickness range thus agrees with Fig. 3(f), where the surface is close to full coalescence at a thickness of $\sim 1.40\,\mu m$, indicating the relation between dislocation and uncoalescence. Okada et al. have shown that the slower annihilation of dislocations led to a reduction in the biaxial strain, dislocation density, and cracks [13], which can be used to explain the relatively low dislocation density obtained in this study, in addition to the reduced thermal stress at lower temperatures [23]. Therefore, the slower annihilation of dislocations was caused by a long transition from 3D to 2D growth modes due to a lower Al-atom mobility as compared to the ones at higher temperatures.

Although interface between the AlN intermediate and buffer layers is hardly distinct in the cross-sectional TEM images as shown in Fig. 5(a–b), the importance of 50-nm thick intermediate layer is shown by growing a two-layer AlN/sapphire structure which excluded the intermediate layer. Otherwise the growth conditions and layer structure of the two-layer AlN/sapphire structure were the same as those of the three-layer AlN/sapphire structure. The $20 \times 20\,\mu m^2$ AFM images in Fig. 6(a–b) show surface morphology of the three-layer and two-layer AlN/sapphire structures. The XRD (002) and (102) FWHMs are also included for comparison.

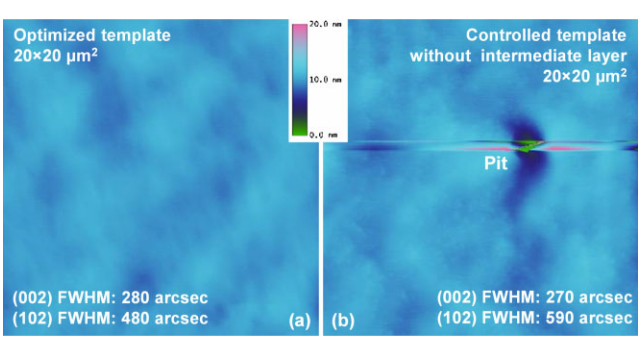

Figure 6 $20 \times 20\,\mu m^2$ AFM images of the (a) three-layer AlN/sapphire structure and (b) two-layer AlN/sapphire structure which excluded the intermediate layer. FWHMs of XRD (002) and (102) ω-scans are included for comparison.

Without the intermediate layer, uncoalesced surface pits with an average density of $\sim 3.75 \times 10^5\,cm^{-2}$ and a lateral dimension of a few micrometers can be seen on the surface of controlled three-layer AlN/sapphire structure, whereas the surface of three-layer AlN/sapphire structure was pit-free. The (002) FWHMs of both AlN/sapphire structures were similar. However, the (102) FWHM of two-layer AlN/sapphire structure is considerably larger than that of the three-layer AlN/sapphire structure. This implies that the higher Al mobility at 1130 °C accelerated 2D growth and thus coalescence of AlN 3D islands, which help annihilate the edge dislocations and thereby reduced the (102) FWHM.

The residual impurity concentrations of carbon (C), hydrogen (H), oxygen (O), and silicon (Si) in the three-layer AlN/sapphire structure were analyzed by SIMS. The result is presented in Table 2 where some previously reported AlN/sapphire data is included for comparison [10, 17, 21, 28]. The C, H, O, and Si concentrations are 8×10^{17}, 4×10^{17}, 1×10^{18}, and 2×10^{16} atoms/cm^3, which are comparable with those of the AlN layers grown at significantly higher temperatures. However, it is noted that the impurity concentrations were found to decrease considerably with higher temperatures in a number of previous studies [10, 17, 21]. Although the decreased impurity concentrations can be caused by an increased evaporation or sublimation rate of impurities from the AlN layers at higher temperatures, the impurity desorption from chamber parts may be enhanced at higher temperatures in the meantime. These two processes can mutually compensate each other. Thus, the impurity concentration should depend on factors including the chamber part composition and temperature. For instance, the AlN growth study carried by Brunner et al. was done in an oxygen-free reactor environment, which avoided O impurity desorption from the chamber parts [10], where the reduction of O impurity with higher temperatures was likely due to the enhanced evaporation or sublimation of impurities from the AlN layers. In this study, the chamber contained a quartz liner surrounding the susceptor, which can introduce O impurities at higher temperatures. This can explain the comparable oxygen impurity concentrations of the AlN layers grown at 1100 and 1300 °C in the same growth chamber between this study and our previous study [28], respectively, as shown in Table 2.

In a separate study, AlGaN-based multiple-quantum-well (MQW) laser heterostructures for optical pumping experiments were grown on the AlN/sapphire structures similar to those reported here. Stimulated emission was observed at wavelengths of 256 and 249 nm with thresholds of 61 and 95 kW/cm^2 at room temperature, respectively, and the internal quantum efficiency (IQE) was 30–56% at 300 K determined by temperature-dependent PL studies [29]. These thresholds set new records at their respective wavelengths and are comparable to the reportedly lowest threshold from the AlGaN-based MQW lasers grown on bulk AlN substrates emitting at 266 nm, which demonstrates the application potential of the three-layer AlN/sapphire structure grown at relatively low temperatures.

Table 2 Concentrations of residual impurities including C, H, O, and Si in the AlN template layer analyzed by SIMS. NA stands for that the data is non-available.

reference	growth temperature (°C)	C (atoms/cm^3)	H (atoms/cm^3)	O (atoms/cm^3)	Si (atoms/cm^3)
this work	1100	8×10^{17}	4×10^{17}	1×10^{18}	2×10^{16}
Ref. [17]	1600	4×10^{16}	7×10^{17}	1×10^{18}	2×10^{18}
Ref. [10]	1500	NA	NA	5×10^{17}	1×10^{17}
Ref. [10]	1400–1300	NA	NA	$1–10 \times 10^{19}$	NA
Ref. [28]	1300	1×10^{17}	9×10^{17}	9×10^{17}	NA
Ref. [21]	1300–1200	2×10^{18}	2×10^{18}	7×10^{17}	NA
Ref. [21]	1100	2×10^{18}	4×10^{18}	1×10^{19}	NA
Ref. [17]	1100	3×10^{17}	2×10^{19}	8×10^{19}	3×10^{18}

4 Conclusions A three-layer planar heteroepitaxial AlN/sapphire structure which comprised a 15-nm thick buffer layer, a 50-nm thick intermediate layer, and a 3.4-μm thick template layer were grown at relatively low temperatures of 930, 1130, and 1100 °C, respectively. The importance of thin intermediate layer was shown by a controlled experiment where the intermediate layer grown at 1130 °C was found to promote 2D growth to prevent surface pits from uncoalesced islands and reduce edge dislocation. The total dislocation density of template layer near the surface was 2.5×10^9/cm^2 determined by TEM, which is comparable to some recently reported planar AlN layers grown on sapphire substrates at temperatures above 1300 °C. In addition, the 20×20 and 1×1 μm^2 AFM scans show low RMS roughness values of 0.50 and 0.07 nm with step terraces, respectively. The relatively low dislocation density and smooth surfaces were attributed to low thermal stress and decreased biaxial strain because of slower dislocation annihilation. The PL measurements exhibited strong and narrow band-edge emission from the surface. The impurity concentrations were relatively low and comparable to those of the AlN layers grown at higher temperatures believed to be due in part to reduced impurity desorption from the chamber parts at relatively low growth temperatures. Because the highest growth temperature was 1130 °C for a relatively short period of time and the sample comprised a simple three-layer structure without the use of PALE or ELO, the growth condition of this study is transferrable to most of the modern MOCVD systems.

Acknowledgements RDD acknowledges the support of Steve W. Chaddick Endowed Chair in Electro-Optics and Georgia Research Alliance. The authors appreciate beneficial discussion with Professor Parbrook and his group at Tyndall National Institute, University College Cork.

References

[1] Z. Lochner, T. T. Kao, Y. S. Liu, X. H. Li, Md. M. Satter, S. C. Shen, P. D. Yoder, J. H. Ryou, R. D. Dupuis, Y. Wei, H. Xie, A. Fischer, and F. A. Ponce, Appl. Phys. Lett. **102**, 101110 (2013).

[2] M. Kneissl, T. Kolbe, C. Chua, V. Kueller, N. Lobo, J. Stellmach, A. Knauer, H. Rodriguez, S. Einfeldt, Z. Yang, N. M. Johnson, and M. Weyers, Semicond. Sci. Technol. **26**, 1 (2011).

[3] H. Hirayama, S. Fujikawa, N. Noguchi, J. Norimatsu, T. Takano, K. Tsubaki, and N. Kamata, Phys. Status Solidi A **206**, 1176 (2009).

[4] U. Zeimer, V. Kueller, A. Knauer, A. Mogilatenko, M. Weyers, and M. Kneissl, J. Cryst. Growth **377**, 32 (2013).

[5] H. Hirayama, S. Fujikawa, J. Norimatsu, T. Takano, K. Tsubaki, and N. Kamata, Phys. Status Solidi C **6**(S2), S356 (2009).

[6] M. Imura, K. Nakano, G. Narita, N. Fujimoto, N. Okada, K. Balakrishnan, M. Iwaya, S. Kamiyama, H. Amano, I. Akasaki, T. Noro, T. Takagi, and A. Bandoh, J. Cryst. Growth **298**, 257 (2007).

[7] Z. Chen, R. S. Q. Fareed, M. Gaevski, V. Adivarahan, J. W. Yang, J. Mei, F. A. Ponce, and M. A. Khan, Appl. Phys. Lett. **89**, 081905 (2006).

[8] Q. Paduano and D. Weyburne, Jpn. J. Appl. Phys. **44**, 4 (2005).

[9] Z. Chen, S. Newman, D. Brown, R. Chung, S. Keller, U. K. Mishra, S. P. Denbaars, and S. Nakamura, Appl. Phys. Lett. **93**, 191906 (2008).

[10] F. Brunner, H. Protzmann, M. Heuken, A. Knauer, M. Weyers, and M. Kneissl, Phys. Status Solidi C **5**, 1799 (2008).

[11] O. Reentila, F. Brunner, A. Knauer, A. Mogilatenko, W. Neumann, H. Protzmann, M. Heuken, M. Kneissl, M. Weyers, and G. Trankle, J. Cryst. Growth **310**, 4932 (2008).

[12] M. Imura, K. Nakano, N. Fujimoto, N. Okada, K. Balakrishnan, M. Iwaya, S. Kamiyama, H. Amano, I. Akasaki, T. Noro, T. Takagi, and A. Bandoh, Jpn. J. Appl. Phys. **46**, 1 (2007).

[13] N. Okada, N. Kato, S. Sato, T. Sumii, T. Nagai, N. Fujimoto, M. Imura, K. Balakrishnan, M. Iwaya, S. Kamiyama, H. Amano, I. Akasaki, H. Maruyama, T. Takagi, T. Noro, and A. Bandoh, J. Cryst. Growth **298**, 349 (2007).

[14] M. Imura, K. Nakano, T. Kitano, N. Fujimoto, N. Okada, K. Balakrishnan, M. Iwaya, S. Kamiyama, H. Amano, I. Akasaki, K. Shimono, T. Noro, T. Takagi, and A. Bandoh, Phys. Status Solidi A **203**, 1626 (2006).

[15] M. L. Nakarmi, B. Cai, J. Y. Lin, and H. X. Jiang, Phys. Status Solidi A **209**, 1 (2012).

[16] N. Fujimoto, T. Kitano, G. Narita, N. Okada, K. Balakrishnan, M. Iwaya, S. Kamiyama, H. Amano, I. Akasaki, K. Shimono, T. Noro, T. Takagi, and A. Bandoh, Phys. Status Solidi C **3**, 6 (2006).

[17] M. Imura, H. Sugimura, N. Okada, M. Iwaya, S. Kamiyama, H. Amano, I. Akasaki, and A. Bandoh, J. Cryst. Growth **310**, 2308 (2008).
[18] S. Hearne, E. Chason, J. Han, J. A. Floro, J. Figiel, J. Hunter, H. Amano, and I. S. T. Tsong, Appl. Phys. Lett. **74**, 356 (1999).
[19] V. Hoffmann, A. Knauer, C. Brunner, S. Einfeldt, M. Weyers, G. Trankle, K. Haberland, J.-T. Zettler, and M. Kneissl, J. Cryst. Growth **315**, 5 (2011).
[20] Naofumi. Kato, S. Sato, H. Sugimura, T. Sumii, N. Okada, M. Imura, M. Iwaya, S. Kamiyama, H. Amano, I. Akasaki, H. Maruyama, T. Takagi, and A. Bandoh, Phys. Status Solidi C **5**, 6 (2008).
[21] A. Kakanakova-Georgieva, D. Nilsson, and E. Janzén, J. Cryst. Growth **338**, 52 (2012).
[22] J. P. Zhang, H. M. Wang, W. H. Sun, V. Adivarahan, S. Wu, A. Chitnis, C. Q. Chen, M. Shatalov, E. Kuokstis, J. W. Yang, and M. Asif Khan, J. Electron Mater. **32**, 5 (2003).
[23] X. H. Li, Y. O. Wei, S. Wang, H. Xie, T. T. Kao, Md. M. Satter, S. C. Shen, P. D. Yoder, T. Detchprohm, R. D. Dupuis, A. Fischer, and F. A. Ponce, J. Cryst. Growth (2014), DOI: 10.1016/j.jcrysgro.2014.10.007.
[24] Y. Wu, A. Hanlon, J. F. Kaeding, R. Sharma, P. T. Fini, S. Nakamura, and J. S. Speck, Appl. Phys. Lett. **84**, 912 (2004).
[25] A. Kakanakova-Georgieva, R. R. Ciechonski, U. Forsberg, A. Lundskog, and E. Janzen, Cryst. Growth Des. **9**(2), 880 (2009).
[26] A. Rice, R. Collazo, J. Tweedie, R. Dalmau, S. Mita, J. Xie, and Z. Sitar, J. Appl. Phys. **108**, 043510 (2010).
[27] B. N. Pantha, R. Dahal, M. L. Nakarmi, N. Nepal, J. Li, J. Y. Lin, H. X. Jiang, Q. S. Paduano, and D. Weyburne, Appl. Phys. Lett. **90**, 241101 (2007).
[28] X. H. Li, J. H. Ryou, T. Detchprohm, and R. D. Dupuis, unpublished, wherein the AlN layer was grown under similar conditions as the AlN template layer in this paper except that the growth temperature was 1300 °C.
[29] X. H. Li, T. Detchprohm, T. T. Kao, Md. M. Satter, S. C. Shen, P. D. Yoder, R. D. Dupuis, S. Wang, Y. O. Wei, H. Xie, A. Fischer, F. A. Ponce, T. Wernicke, C. Reich, M. Martens, and M. Kneissl, Appl. Phys. Lett. **105**, 141106 (2014).